

UC Davis

UC Davis Previously Published Works

Title

Vaccine-Boosted CCP Decreases Virus Replication and Hastens Resolution of Infection Despite Transiently Enhancing Disease in SARS-CoV-2–Infected Hamsters

Permalink

<https://escholarship.org/uc/item/3mp1s3hw>

Journal

The Journal of Infectious Diseases, 229(6)

ISSN

0022-1899

Authors

Carroll, Timothy D

Wong, Talia

Morris, Mary Kate

et al.

Publication Date

2024-06-14

DOI

10.1093/infdis/jiad568

Peer reviewed

Vaccine-Boosted CCP Decreases Virus Replication and Hastens Resolution of Infection Despite Transiently Enhancing Disease in SARS-CoV-2–Infected Hamsters

Timothy D. Carroll,^{1,2} Talia Wong,¹ Mary Kate Morris,³ Clara Di Germanio,⁴ Zhong-min Ma,² Mars Stone,^{4,6} Erin Ball,¹ Linda Fritts,^{1,2} Arjun Rustagi,⁵ Graham Simmons,⁴ Michael Busch,⁴ and Christopher J. Miller^{1,2,6}

¹Department of Pathology, Microbiology, and Immunology, School of Veterinary Medicine, University of California Davis, Davis, California, USA; ²California National Primate Research Center, University of California Davis, Davis, California, USA; ³Division of Viral and Rickettsial Diseases, California Department of Public Health, Richmond, California, USA; ⁴Vitalant Research Institute, San Francisco, California, USA; ⁵Division of Infectious Diseases and Geographic Medicine, Department of Medicine, Stanford University School of Medicine, Palo Alto, California, USA; and ⁶Division of Infectious Diseases, Department of Internal Medicine, School of Medicine, University of California Davis, Sacramento, California, USA

Definitive data demonstrating the utility of coronavirus disease 2019 (COVID-19) convalescent plasma (CCP) for treating immunocompromised patients remains elusive. To better understand the mechanism of action of CCP, we studied viral replication and disease progression in severe acute respiratory syndrome coronavirus 2 (SARS-CoV-2)–infected hamsters treated with CCP obtained from recovered COVID-19 patients that were also vaccinated with an mRNA vaccine, hereafter referred to as Vaxplas. Vaxplas transiently enhanced disease severity and lung pathology in hamsters treated near peak viral replication due to immune complex and activated complement deposition in pulmonary endothelium, and recruitment of M1 proinflammatory macrophages into the lung parenchyma. However, aside from one report, transient enhanced disease has not been reported in CCP recipient patients, and the transient enhanced disease in Vaxplas hamsters may have been due to mismatched species IgG-FcR interactions, infusion timing, or other experimental factors. Despite transient disease enhancement, Vaxplas dramatically reduced virus replication in lungs and improved infection outcome in SARS-CoV-2–infected hamsters.

Keywords. COVID-19; transfusion; immune plasma; animal models.

Beginning in fall 2019, in China and then worldwide, a novel respiratory disease, coronavirus disease 2019 (COVID-19), was seen in a subset of people infected with the severe acute respiratory syndrome coronavirus 2 (SARS-CoV-2) [1]. Due to the historical success of convalescent plasma in treatment of other viral diseases, infusion of COVID-19 convalescent plasma (CCP) obtained from recovered COVID-19 patients was tested early in the pandemic [2–4]. CCP with high-titer neutralizing antibodies, administered within 72 hours of symptom onset, decreases disease progression, hospitalization, and mortality [5, 6]. While anti-spike (anti-S) monoclonal antibodies were used to successfully treat COVID-19 early in the pandemic, more transmissible,

monoclonal antibody-resistant SARS-CoV-2 variants have emerged as SARS-CoV-2 has evolved [7–12]. In contrast, CCP obtained from patients recovering from currently circulating SARS-CoV-2 variants maintains clinical efficacy against emerging SARS-CoV-2 variants [13, 14]. In January 2022, the Food and Drug Administration (FDA) revised the Emergency Use Authorization of CCP to include patients who are hospitalized with impaired humoral immunity [15]. One randomized trial reported improved survival of immunosuppressed patients given CCP despite transient worsening of pulmonary function 4 days after the infusion [16]; however, other studies have not reported enhanced disease [17, 18].

To understand CCP's mechanism of action, we studied viral replication and disease progression in SARS-CoV-2–infected hamsters treated with CCP obtained from recovered patients subsequently vaccinated with an mRNA vaccine, hereafter referred to as Vaxplas, or unvaccinated individuals that had recovered from infection (CCP). We found that Vaxplas dramatically reduced virus replication in the lungs and reduced disease severity in SARS-CoV-2–infected hamsters.

METHODS

Ethics Statement

All animal experiments were approved by the Institutional Animal Care and Use Committee of University of California

Received 25 July 2023; editorial decision 17 October 2023; accepted 05 December 2023; published online 12 January 2024

Presented in part: Association for the Advancement of Blood and Biotherapies meeting, Memphis, TN, 12–15 October 2023, poster presentation.

Correspondence: Christopher J. Miller, DVM, PhD, California National Primate Research Center, University of California Davis, One Shields Avenue, Davis, CA 95616 (cjmiller@ucdavis.edu); Timothy Carroll, PhD, Department of Pathology, Microbiology, and Immunology, School of Veterinary Medicine, University of California Davis, One Shields Avenue, Davis, CA 95616 (tdcarroll@ucdavis.edu).

The Journal of Infectious Diseases® 2024;229:1702–10

© The Author(s) 2024. Published by Oxford University Press on behalf of Infectious Diseases Society of America. All rights reserved. For permissions, please e-mail: journals.permissions@oup.com

<https://doi.org/10.1093/infdis/jiad568>

Davis (protocol No. 22233) and performed following the guidelines and basic principles in the United States Public Health Service Policy on Humane Care and Use of Laboratory Animals and the Guide for the Care and Use of Laboratory Animals. The work with infectious SARS-CoV-2 under biosafety level 3 conditions was approved by the University of California Davis Institutional Biosafety Committee.

Human Plasma

Plasma pools made from aliquots of frozen plasma collected from human donors were used. Details of the control pool of normal plasma containing no anti-SARS-CoV-2 antibodies and CCP pool have been provided in previously published studies [19, 20]. The CCP pool had a 50% neutralization titer (NT₅₀) of 1149 in a reporter virus assay [21]. The Vaxplas plasma pool was made by combining plasma aliquots from 3 individual donors that had been vaccinated after recovering from a documented SARS-CoV-2 infection to achieve a pool that had a NT₅₀ of 9901 in a reporter virus assay [21]. Two of the 3 Vaxplas pool donors were immunized with 2 doses of the FDA EUA-approved, monovalent Moderna vaccine and 1 donor was immunized with 2 doses of the FDA EUA-approved, monovalent Pfizer vaccine. The interval between the second immunization and plasma donations was between 2 and 6 months.

Hamsters

Male, 7–9-week-old Syrian hamsters purchased from Charles River, Inc were infused intraperitoneally with 2 mL plasma.

Viruses and Cells

SARS-CoV-2 variants were isolated from patient swabs by California Department of Public Health, Richmond, CA and Stanford University, Palo Alto, CA, and sequence verified as previously described [22].

Hamster Inoculations

For experimental inoculations, hamsters were infected intranasally with a total dose of variant mixture containing approximately 5000 plaque-forming unit (PFU) of SARS-CoV-2 suspended in 50 µL sterile Dulbecco's Modified Eagle's Medium as previously described [22]. The dose of all variants was approximately equal (<10-fold difference).

qPCR for Subgenomic RNA Quantitation

Quantitative real-time polymerase chain reaction (PCR) assays were developed for detection of full-length genomic viral RNA (gRNA), subgenomic viral RNA (sgRNA), and total viral RNA as previously described [22].

Histopathology

At necropsy, lungs were evaluated blindly by a board-certified veterinary anatomic pathologist (T.W.) blindly and the area of

inflamed tissue (visible to the naked eye at subgross magnification) was estimated as a percentage of the total surface area of the lung section. The scores for healthy normal hamsters were set at zero.

Immunohistochemistry and Immunofluorescence Staining of Lung Sections

Rabbit monoclonal (EPR4421) anti-human IgG (Abcam), rabbit polyclonal anti-C3/C3b (EnenTex), mouse monoclonal (GT10312) anti-IBA1 (Invitrogen), and rabbit monoclonal (Tyr701) (58D6) anti-phospho-Stat1 (Cell Signaling) antibodies were used. Briefly, 5 µm paraffin sections were subjected to an antigen-retrieval step consisting of incubation in AR10 (Biogenex) for 2 minutes at 125°C in the Digital Decloaking Chamber (Biocare), followed by cooling to 90°C for 10 minutes. The EnVision detection system (Agilent) was used with 3-amino-9-ethylcarbazole (Agilent) as the chromogen. Slides were counterstained with Gill's hematoxylin I (StatLab). Primary antibodies were replaced by mouse or rabbit isotype control (Thermo Fisher) and run with each staining series as the negative controls. In the double immunofluorescent stains of IBA1 and phospho-Stat1, goat anti-mouse Alexa Fluor 488 and goat anti-rabbit Alexa Fluor 568 (Invitrogen) were used to detect bound primary antibodies.

Quantitation of Human IgG by ELISA

Total human immunoglobulin G (IgG) levels were determined following the manufacturer's instructions in the Human IgG Total ELISA Kit (Invitrogen).

Quantitation of Anti-Spike Antibody Levels

Anti-S IgG levels were measured on the Ortho VITROS platform (Ortho Clinical Diagnostics) at Vitalant Research Institute as described [23]. Samples were tested following the manufacturer's instructions, except that samples with results above the limit of quantitation of >200 binding antibody unit (BAU)/mL were further tested at 1:20 dilution.

Statistical Analysis

As noted in figure legends, median values were compared using the nonparametric Kruskal-Wallis and a post-hoc Dunn multiple comparison test, or Mann-Whitney test was used for pairwise comparisons of the groups. Although comparisons between all groups were made, for the sake of clarity, we have denoted only significant differences in the figures. For all analyses, differences with a *P* value < .05 were considered significant. Graph Pad Prism 9.3.1 installed on a MacBook Pro running Mac OS Monterey version 12.1 was used for the analysis.

RESULTS

Human IgG and Anti-Spike Binding Antibody Levels in Hamsters Infused With Human Plasma

Forty male, 8–10-week-old Syrian golden hamsters were intranasally inoculated with 5000 PFU of a mixture of 7

Table 1. SARS-CoV-2 Variants Used to Produce the Mixed Inoculum for These Studies

WHO Variant Group	Strain ID	Origin	GISAID Number	Target PFU/50 μ L
Ancestral	614G	CDPH 20/238 2021-02-04	...	725
Alpha	B.1.1.7	CDPH 20/363 2021-03-16	...	725
Beta	B.1.351	Stanford VOC16 P2 2021-03-21	EPI_ISL_1335872	725
Gamma	P.1	CDPH 21/66 2021-07-06	...	725
Delta	B.1.617.2	CDPH 21/909 2021-06-03	...	725
Epsilon	B.1.429	CDPH 20/917 2021-03-16	CA-CDPH309-P1	725
Epsilon	B.1.427	CDPH 20/070 2021-02-04	CA-CDPH309-P1	725

Abbreviations: CDPH, California Department of Public Health; PFU, plaque-forming unit; SARS-CoV-2, severe acute respiratory syndrome coronavirus 2; WHO, World Health Organization.

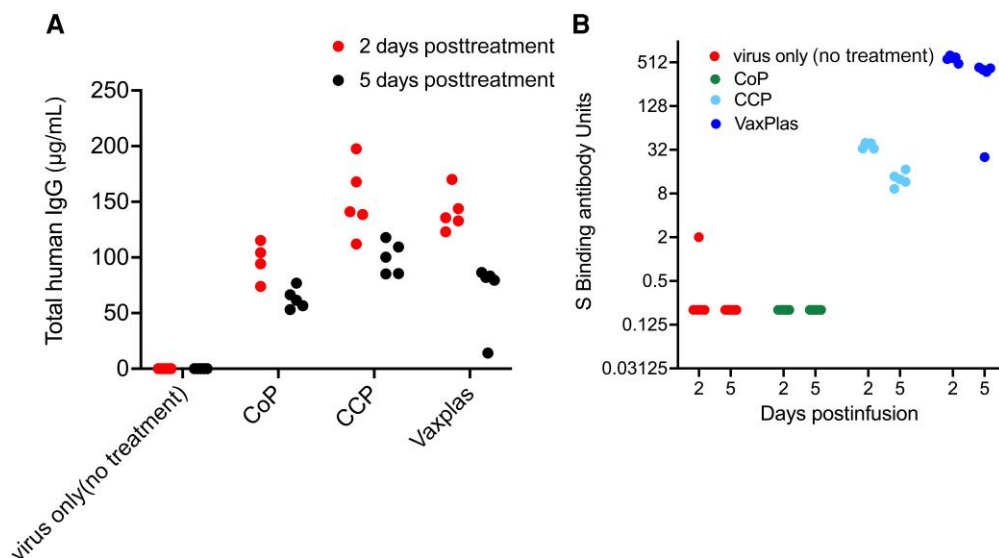


Figure 1. Human IgG levels and spike binding antibody levels in hamsters infused with human plasma after SARS-CoV-2 infection. *A*, Levels of human IgG in the blood of hamsters collected 2 and 5 days after intraperitoneal infusion of Vaxplas, CCP, and CoP. *B*, Levels of anti-spike binding antibodies in the blood of hamsters collected 2 and 5 days after plasma infusion. Abbreviations: CCP, coronavirus disease 2019 convalescent plasma; CoP, control plasma; IgG, immunoglobulin G.

SARS-CoV-2 strains (Table 1). Our rationale for using a mixed inoculum of 7 SARS-CoV-2 variants was to determine if replication of a particular variant in the mixture was more resistant to immune control by CCP and Vaxplas than other variants. However technical issues with the Quills assay [22] has delayed that analysis indefinitely.

Twenty-four hours after the virus inoculation, groups of 10 hamsters were infused by peritoneal injection with 2 mL of Vaxplas, or CCP from unvaccinated, convalescent COVID-19 patients, or control plasma (CoP) from SARS-CoV-2-naive human donors, and a fourth group of 10 hamsters was untreated. To assess lung histology and viral loads, 5 animals from each group were necropsied at day 3 postinfection (PI) near the peak of virus replication [22], and the remaining animals were necropsied at day 6 PI when virus replication in lungs is largely undetectable [22].

Two days after the infusions (day 3 PI) of the Vaxplas, CCP, and CoP animals, human IgG levels in plasma exceeded 50 μ g/mL (range, 74–197 μ g/mL; Figure 1A). As expected, human

IgG was undetectable in the virus-only animals (Figure 1A). Five days after the infusions (day 6 PI), human IgG levels had declined (range, 14–117 μ g/mL) in plasma of the Vaxplas, CCP, and CoP hamsters (Figure 1A). Human IgG was undetectable in the virus-only animals at day 6 PI (Figure 1A). These results demonstrate the successful transfer of human IgG to the treated animals.

Two days after the infusions (day 3 PI), anti-S antibody levels were high (>512 S BAU) in the Vaxplas group, moderate (30–40 S BAU/mL) in the CCP group, but aside from 1 animal, undetectable in the CoP and virus-only group. It is unclear why one virus-only animals had very low levels of S antibodies (2 S BAU/mL; Figure 1B). Five days after the infusions (day 6 PI), anti-S antibody levels were moderate to high (range 32–512 S BAU/mL) in the Vaxplas group, low (9–17 BAU/mL) in the CCP group, and undetectable in the CoP and virus-only group (Figure 1B). Thus, anti-SARS-CoV-2 spike IgG binding antibodies were transferred by the infusions of CCP and Vaxplas, and the Vaxplas animals had at least 10-fold higher anti-S IgG antibody levels than the CCP group.

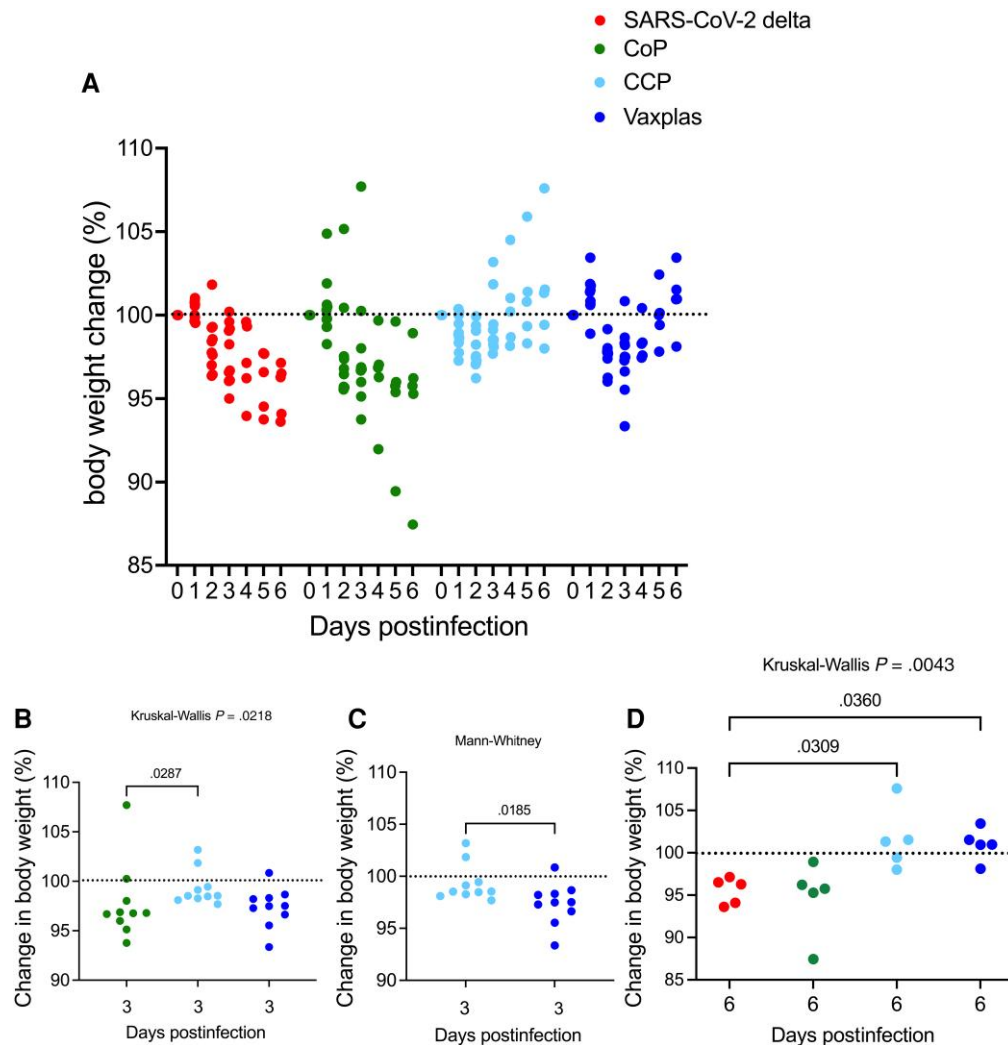


Figure 2. Percent BWC in hamsters infused with human plasma after SARS-CoV-2 infection. *A*, Comparison of daily change in body weight (%) in treated and virus-only hamsters after SARS-CoV-2 infection. *B*, Comparison of BWC in treated hamsters 3 days after SARS-CoV-2 infection. *C*, Comparison of BWC in CCP- and Vaxplas-treated hamsters 3 days after SARS-CoV-2 infection. *D*, Comparison of BWC in treated hamsters 6 days after SARS-CoV-2 infection. *B* and *D*, Kruskal-Wallis test with pairwise comparisons. *C*, Mann-Whitney test. Abbreviations: BWC, body weight change; CCP, coronavirus disease 2019 convalescent plasma; CoP, control plasma; SARS-CoV-2, severe acute respiratory syndrome coronavirus 2.

Effect of CCP on Disease Severity

We used change in body weight to assess disease severity in the infected animals. Body weight transiently declined in all the hamsters inoculated with SARS-CoV-2. The greatest body weight declines occurred in the virus-only and CoP-treated animals at day 6 PI. Body weights were lowest in CCP-treated animals at day 2 PI and at day 3 in the Vaxplas-treated animals but had not declined further by day 6 (Figure 2A). At day 3 PI, the differences in body weight change (BWC) between the CoP, CCP, and Vaxplas groups were significant, with the CoP animals having more severe weight loss than the CCP animals at day 3 PI (Figure 2B). In addition, at day 3 PI, the Vaxplas animals had more severe weight loss than the CCP animals (Figure 2C). At days 6 PI, the extent of the BWC in the virus-only and CoP groups

were similar and significantly greater than in the CCP and Vaxplas groups (Figure 2D). These results establish that the CCP- and Vaxplas-treated animals had less severe disease than the untreated or CoP-treated hamsters at day 6 PI. Unexpectedly, at day 3 PI, the CCP group had significantly greater BWC than the CoP group (Figure 2B) and the Vaxplas-treated animals had significantly more BWC than the CCP group (Figure 2C).

Effect of CCP on Virus Replication

At day 3 PI, the levels of sgRNA in the upper respiratory tract (URT) were very high ($>10^6$ copies/ μ g total RNA) in all 4 animal groups (Figure 3A). At day 6 PI, sgRNA levels in the URT were lower and more variable ($<10^6$ copies/ μ g total RNA in about 50% of animals) in all 4 animal groups

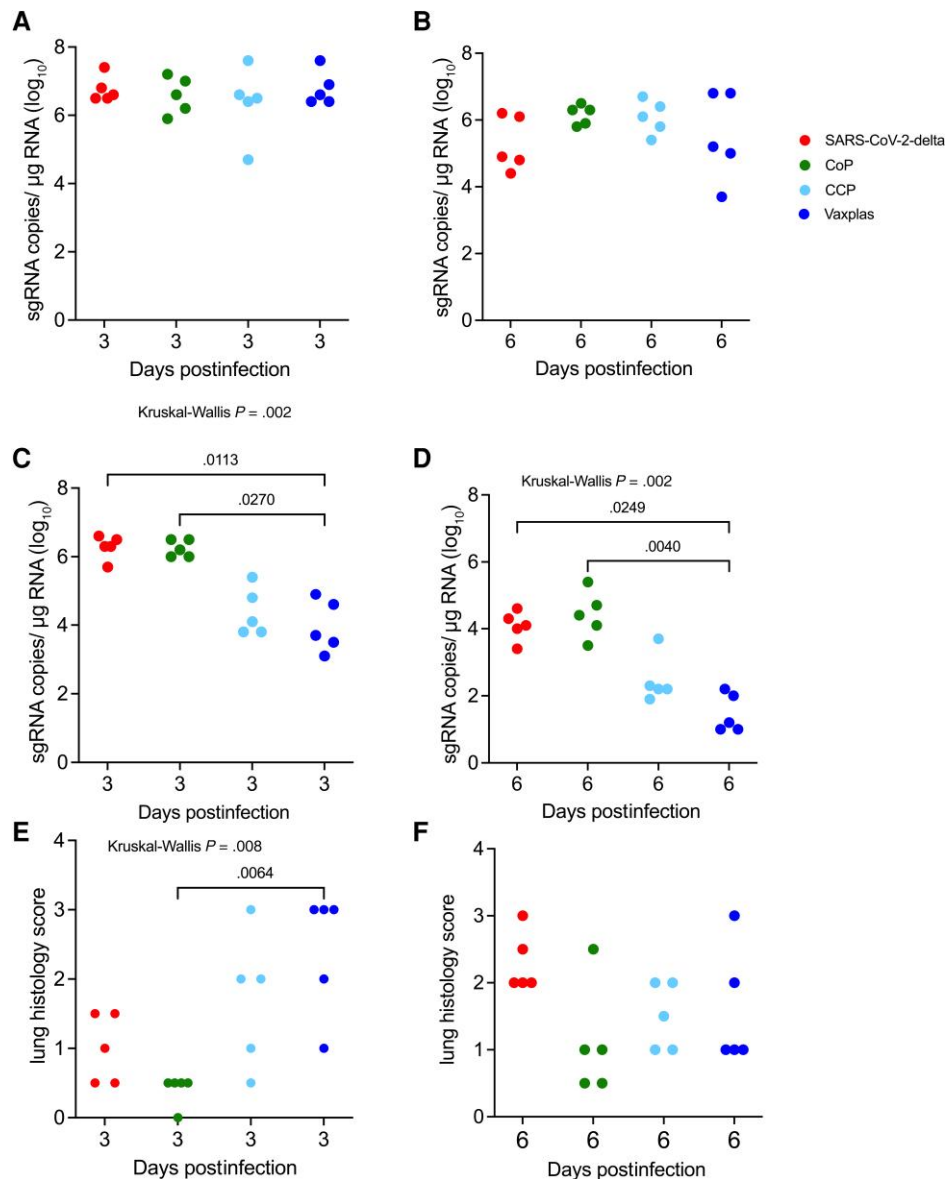


Figure 3. Virology and lung histopathology scores in hamsters infused with human plasma after SARS-CoV-2 infection. Comparison of sgRNA levels in (A) URT of treated and control hamsters 3 days postinfection; (B) URT of treated and control hamsters 6 days postinfection; (C) lungs of treated and control hamsters 3 days postinfection; and (D) lungs of treated and naive control hamsters 6 days postinfection. Comparison of lung histopathology scores of treated and control hamsters at (E) 3 days and (F) 6 days postinfection. A–F, Kruskal-Wallis test with pairwise comparisons. Abbreviations: CCP, coronavirus disease 2019 convalescent plasma; CoP, control plasma; URT, upper respiratory tract; SARS-CoV-2, severe acute respiratory syndrome coronavirus 2; sgRNA, subgenomic RNA.

(Figure 3B). Thus, CCP and Vaxplas had little effect on virus replication in the URT.

At day 3 PI, the virus-only and CoP animals had high levels of sgRNA in lungs (Figure 3C), while the CCP- and Vaxplas-treated animals had lower sgRNA in lungs (Figure 3C). Pairwise comparison demonstrated that the difference in sgRNA levels in lungs of Vaxplas-treated animals compared to CoP-treated and virus-only animals was significant (Figure 3C). At day 6 PI, sgRNA levels were significantly different in the lungs of the 4 animal groups (Figure 3D). These demonstrate that Vaxplas and CCP blunt SARS-CoV-2 replication

in the lungs but not the URT of SARS-CoV-2-infected hamsters.

Effect of CCP on Lung Pathology

The lungs of the animals were evaluated histologically, and the total area of diseased lung was estimated and scored. In the virus-only and CoP animal groups, lung lesions were less extensive at 3 days PI and more extensive at 6 days PI (Figure 3E and 3F), while in the CCP and Vaxplas groups lung lesions were more extensive at 3 days PI and less extensive at 6 days PI (Figure 3E and 3F). At day 3 PI the differences in

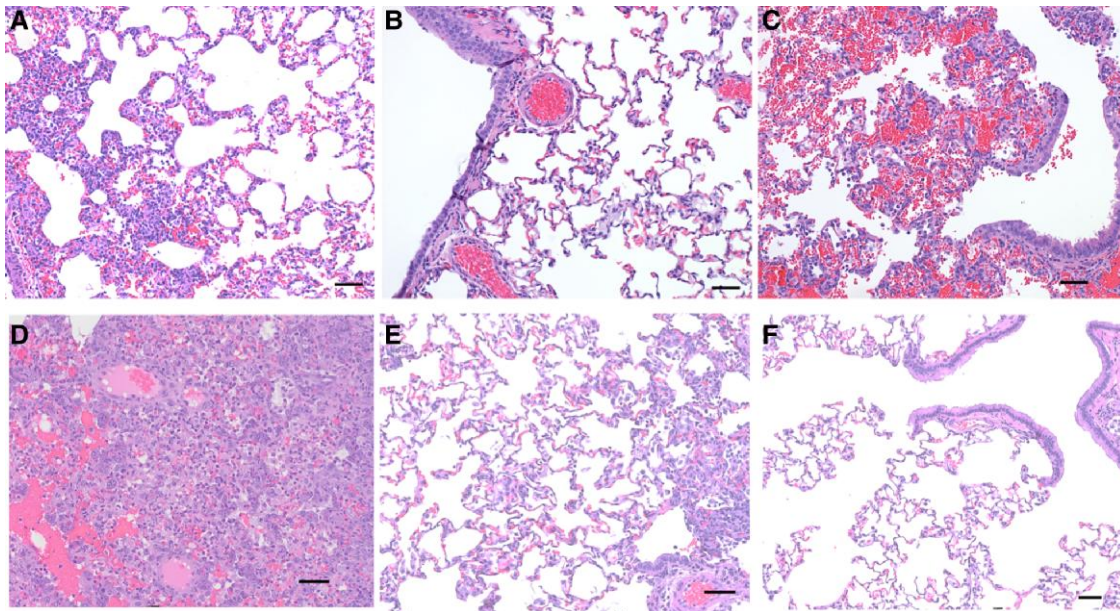


Figure 4. Histopathology of lungs of hamsters infused with human plasma after SARS-CoV-2 infection. A–C, Day 3 postinfection: (A) virus-only animals, (B) control plasma (CoP) animals, and (C) Vaxplas animals. D–F, Day 6 postinfection: (D) virus-only animals, (E) CoP animals, and (F) Vaxplas animals. G–I, IBA1⁺ cells in (G) virus-only animals, (H) CoP animals, and (I) Vaxplas animals. Hematoxylin and eosin stain. Scale bars = 50 μ m.

the extent of lung disease among the groups were significant, and pairwise comparison demonstrated that there was significantly more disease in the Vaxplas group compared to the CoP group (Figure 3E). At day 6 PI, lung disease was most widespread in the virus-only group, lowest in the CoP group and intermediate in the CCP and Vaxplas groups, although the differences among the groups were not significant due to considerable intergroup variability (Figure 3F).

The nature of the lesions in the virus-only, CoP-, and CCP-treated animals were similar and consistent with previous reports [22, 24]. At day 3 PI, these 3 groups had moderate multifocal necrosuppurative bronchiolitis (Figure 4A and 4B) with perivascular lymphocytic cuffing and endotheliitis in small arteries. Variable bronchiolar epithelial hyperplasia and scattered type II pneumocyte hyperplasia were also noted. The changes in the lungs of the Vaxplas animals at day 3 PI (loss of alveolar septal architecture, hemorrhage, edema, fibrin, necrotic debris, and mixed inflammation, perivascular cuffing, and endotheliitis) were more severe and extensive than in the other groups (Figure 4C). At day 6 PI, animals in all groups had necrotizing, neutrophilic, and histiocytic bronchointerstitial pneumonia with syncytial cells, perivascular cuffing, and endotheliitis, with prevalent bronchiolar epithelial hyperplasia and type II pneumocyte hyperplasia (Figure 4D–F). However, at day 6 the inflammation and hemorrhage in the Vaxplas animals had resolved to a greater extent than the other groups.

In day 3 PI lung sections of virus-only animals, human IgG was undetectable but the C3 complement fragment was found in the lumen and walls of small and medium blood vessels and

capillaries within alveolar septa (Figure 5A and 5D). In the CCP and Vaxplas animals, human IgG and C3 were localized in the medium-size blood vessels and in alveolar septa capillaries (Figure 5B, 5C, 5E, and 5F). In the CoP animals, human IgG and C3 were found only in the lumen and walls of medium and small blood vessels with little staining in alveolar septa capillaries (Figure 5B and 5E). In the Vaxplas animals, extravascular human IgG and C3 were also found in the alveolar spaces and inflamed areas of the pulmonary parenchyma (Figure 5C and 5F).

In day 3 PI lung sections of all animals, variable numbers of IBA1⁺ macrophages were found in and around inflamed airways and blood vessels, and in inflamed alveolar septa and alveolar spaces (Figure 5G–I). The number of IBA1⁺ macrophages was highest in the lungs of the Vaxplas (Figure 5I), moderate in the CCP animals and the virus-only animals (Figure 5G) and lowest in the CoP animals (Figure 5H). Double-label immune fluorescent staining demonstrated that >90% of IBA1⁺ macrophages were Stat1⁺ (inset, Figure 5I), indicating that most macrophages in the lungs of SARS-CoV-2-infected hamsters, regardless of treatment, had a proinflammatory M1 phenotype. In addition, the numbers of IBA1⁺ [25] and Stat1⁺ [26–28] macrophages in the lungs of Vaxplas animals were significantly higher than in the CoP animals (Figure 6A and 6B) at day 3 PI.

DISCUSSION

We found that Vaxplas infused 24 hours after SARS-CoV-2 infection improved disease outcome in hamsters. Furthermore,

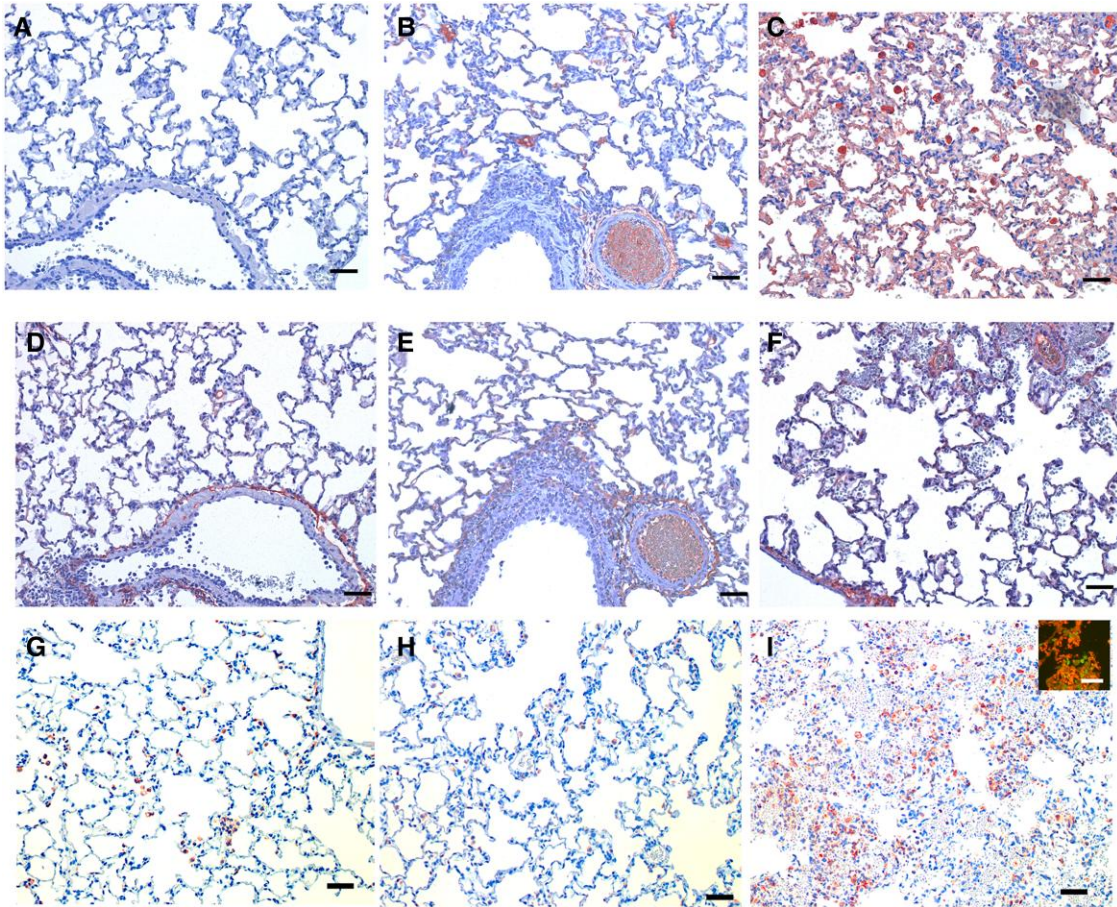


Figure 5. Immunohistochemical staining of human IgG, C3 fragment of complement, and IBA1⁺ macrophages in lungs of hamsters infused with human plasma after SARS-CoV-2 infection. Human IgG staining: (A) virus-only animals, (B) control plasma (CoP) animals, and (C) Vaxplas animals. C3 staining: (D) virus-only animals, (E) CoP animals, and (F) Vaxplas animals. IBA1⁺ cells: (G) virus-only animals, (H) CoP animals, and (I) Vaxplas animals; inset, IBA1 and Stat1 double immunofluorescent staining of macrophages. Hematoxylin counterstain. Scale bars = 50 μ m.

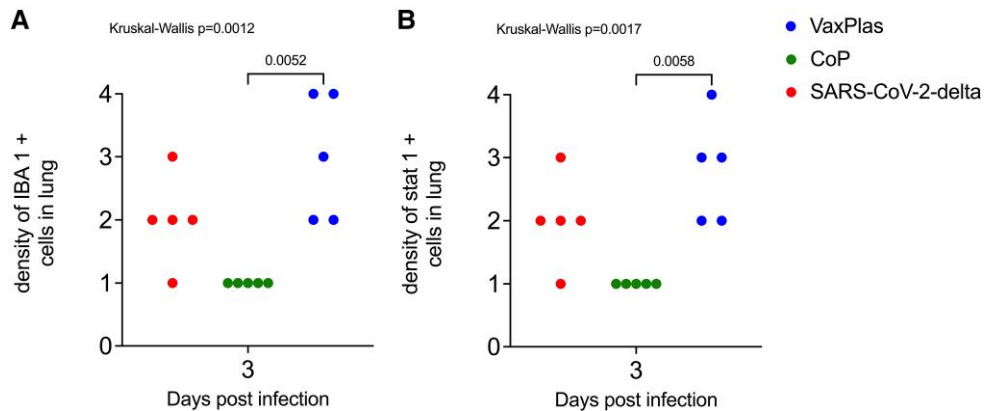


Figure 6. Number of IBA1⁺ macrophages and Stat1⁺ cells in lungs of hamsters infused with human plasma after SARS-CoV-2 infection. A, Comparison IBA1⁺ macrophages in lungs of treated and virus-only hamsters 3 days after SARS-CoV-2 infection. B, Comparison Stat1⁺ cells in lungs of treated and virus-only hamsters 3 days after SARS-CoV-2 infection. A and B, Kruskal-Wallis test with pairwise comparisons; both panels. Abbreviations: CCP, coronavirus disease 2019 convalescent plasma; CoP, control plasma; SARS-CoV-2, severe acute respiratory syndrome coronavirus 2.

Vaxplas dramatically reduced virus replication in the lung, but not the URT, of infected hamsters. Peritoneal infusion of Vaxplas, CCP, and CoP resulted in transfer of human IgG to the hamsters in the range of 50–200 µg/mL (0.5–20 mg/dL) of hamster plasma, a concentration that is about 50 to 100-fold lower than the median IgG levels found in adult humans [29]. Thus, while the plasma infusions successfully transferred human IgG to the hamsters, the dose of human IgG that the animals received was modest. The extent of the reduction in viral replication in these Vaxplas and CCP groups was consistent with the relative amount of anti-S antibodies transferred to the 2 groups of hamsters. Thus, median anti-S antibody titers in the Vaxplas group were approximately 16 times higher than in the CCP group and the median sgRNA levels were 5–10 times lower than in the Vaxplas group compared to the CCP group.

Despite the modest levels of anti-S antibodies transferred to the hamsters, the infusions improved the course of SARS-CoV-2 disease. By the end of the study (6 days PI) both the CCP animals and the Vaxplas animals had significantly less body weight loss than the virus-only animals and there was a similar trend with the CoP group. While this milder disease course was apparent in the CCP animals relative to CoP animals at day 3 PI, it was not apparent in the Vaxplas animals (Figure 2B). In fact, the body weight loss in the Vaxplas animals was significantly greater than in the CCP animals at day 3 PI (Figure 2C), indicating that disease severity was transiently enhanced in Vaxplas animals but not in the CCP group. This enhanced disease occurred even though the Vaxplas animals had the lowest lung viral loads of any animal group at day 3 PI (Figure 3C). The transiently enhanced disease severity and lung pathology in the Vaxplas group was likely due to the deposition of immune complexes, activation of complement, and recruitment of M1 proinflammatory macrophages into the lung parenchyma. Aside from one study [16], enhanced disease has not been reported in humans receiving CCP [17, 18], thus the transient enhanced disease in Vaxplas hamsters may be due to cross-species IgG-FcR interactions, treatment near peak virus replication, or other experimental factors.

At day 3 and 6 PI, while lung sgRNA levels were significantly higher in the CoP group compared to the Vaxplas group, the CoP group had significantly lower lung pathology scores at day 3 and significantly fewer lung Stat1⁺ and IBA1⁺ macrophages in lung parenchyma at day 3 and 6 PI. Thus, it appears that normal human plasma containing no anti-SARS-CoV-2 antibodies reduced lung disease compared to Vaxplas-treated, SARS-CoV-2-infected hamsters, while having no effect on virus replication. Studies should be undertaken to understand the mechanism behind this observation with the hypothesis that the CoP mitigates the pulmonary endotheliopathy, perhaps driven by virus-antibody immune complexes, commonly seen in COVID-19 patients [30] and SARS-CoV-2-infected hamsters [22].

CONCLUSIONS

Infusion of hamsters 24 hours after SARS-CoV-2 infection with moderate-titer CCP and high-titer Vaxplas CCP blunts virus replication in the lungs and improves the course of viral disease. In addition, although normal human plasma has no effect on clinical disease (weight loss) or virus replication in hamsters, it does decrease the severity and extent of inflammation in the lungs compared to Vaxplas infusion.

Notes

Disclaimer. The funders had no role in study design, data collection and analysis, decision to publish, or preparation of the manuscript. The findings and conclusions in this article are those of the authors and do not necessarily represent the views or opinions of the California Department of Public Health or the California Health and Human Services Agency.

Financial support. This work was supported by intramural funding from the Center for Immunology and Infectious Diseases, University of California Davis (grant number CIID-2020-2); Vitalant (grant number A22-2082); and National Institutes of Health (grant number R01-AI118590 to C. J. M.).

Potential conflicts of interest. All authors: No reported conflicts of interest. All authors have submitted the ICMJE Form for Disclosure of Potential Conflicts of Interest. Conflicts that the editors consider relevant to the content of the manuscript have been disclosed.

References

1. World Health Organization. Coronavirus disease (COVID-19) pandemic. <https://www.who.int/emergencies/diseases/novel-coronavirus-2019>. Accessed 23 July 2023.
2. Casadevall A, Pirofski LA. The convalescent sera option for containing COVID-19. *J Clin Invest* **2020**; 130:1545–8.
3. Franchini M, Corsini F, Focosi D, Cruciani M. Safety and efficacy of convalescent plasma in COVID-19: an overview of systematic reviews. *Diagnostics (Basel)* **2021**; 11:1663.
4. Franchini M, Liumbruno GM, Piacentini G, Glingani C, Zaffanello M. The three pillars of COVID-19 convalescent plasma therapy. *Life (Basel)* **2021**; 11:354.
5. Focosi D, Franchini M. COVID-19 convalescent plasma therapy: hit fast, hit hard! *Vox Sang* **2021**; 116:935–42.
6. Focosi D, Franchini M, Pirofski LA, et al. COVID-19 convalescent plasma and clinical trials: understanding conflicting outcomes. *Clin Microbiol Rev* **2022**; 35:e0020021.
7. Pommeret F, Colomba J, Bigenwald C, et al. Bamlanivimab + etesevimab therapy induces SARS-CoV-2 immune escape mutations and secondary clinical deterioration in COVID-19 patients with B-cell malignancies. *Ann Oncol* **2021**; 32:1445–7.

8. Jary A, Marot S, Faycal A, et al. Spike gene evolution and immune escape mutations in patients with mild or moderate forms of COVID-19 and treated with monoclonal antibodies therapies. *Viruses* **2022**; 14:226.
9. Focosi D, McConnell S, Casadevall A, et al. Monoclonal antibody therapies against SARS-CoV-2. *Lancet Infect Dis* **2022**; 22:e311–26.
10. Sheikh A, McMenamin J, Taylor B, et al. SARS-CoV-2 delta VOC in Scotland: demographics, risk of hospital admission, and vaccine effectiveness. *Lancet* **2021**; 397:2461–2.
11. Ong SWX, Chiew CJ, Ang LW, et al. Clinical and virological features of severe acute respiratory syndrome coronavirus 2 (SARS-CoV-2) variants of concern: a retrospective cohort study comparing B.1.1.7 (Alpha), B.1.351 (Beta), and B.1.617.2 (Delta). *Clin Infect Dis* **2022**; 75:e1128–36.
12. Fisman DN, Tuite AR. Evaluation of the relative virulence of novel SARS-CoV-2 variants: a retrospective cohort study in Ontario, Canada. *CMAJ* **2021**; 193:E1619–25.
13. Li M, Beck EJ, Laeyendecker O, et al. Convalescent plasma with a high level of virus-specific antibody effectively neutralizes SARS-CoV-2 variants of concern. *Blood Adv* **2022**; 6:3678–83.
14. Gachoud D, Bertelli C, Rufer N. Understanding the parameters guiding the best practice for treating B-cell-depleted patients with COVID-19 convalescent plasma therapy. *Br J Haematol* **2023**; 200:e25–7.
15. Senefeld JW, Franchini M, Mengoli C, et al. COVID-19 convalescent plasma for the treatment of immunocompromised patients: a systematic review and meta-analysis. *JAMA Netw Open* **2023**; 6:e2250647.
16. Lacombe K, Hueso T, Porcher R, et al. COVID-19 convalescent plasma to treat hospitalised COVID-19 patients with or without underlying immunodeficiency: a randomized trial. doi: [10.1101/2022.08.09.22278329](https://doi.org/10.1101/2022.08.09.22278329). Accepted for publication in *BMJ Medicine*.
17. Avendano-Sola C, Ramos-Martinez A, Munez-Rubio E, et al. A multicenter randomized open-label clinical trial for convalescent plasma in patients hospitalized with COVID-19 pneumonia. *J Clin Invest* **2021**; 131:e15274.
18. RECOVERY Collaborative Group. Convalescent plasma in patients admitted to hospital with COVID-19 (RECOVERY): a randomised controlled, open-label, platform trial. *Lancet* **2021**; 397:2049–59.
19. Van Rompay KKA, Olstad KJ, Sammak RL, et al. Early post-infection treatment of SARS-CoV-2 infected macaques with human convalescent plasma with high neutralizing activity had no antiviral effects but moderately reduced lung inflammation. *PLoS Pathog* **2022**; 18:e1009925.
20. Deere JD, Carroll TD, Dutra J, et al. SARS-CoV-2 infection of rhesus macaques treated early with human COVID-19 convalescent plasma. *Microbiol Spectr* **2021**; 9:e0139721.
21. Di Germanio C, Simmons G, Kelly K, et al. SARS-CoV-2 antibody persistence in COVID-19 convalescent plasma donors: dependency on assay format and applicability to serosurveillance. *Transfusion* **2021**; 61:2677–87.
22. Carroll T, Fox D, van Doremalen N, et al. The B.1.427/1.429 (Epsilon) SARS-CoV-2 variants are more virulent than ancestral B.1 (614G) in Syrian hamsters. *PLoS Pathog* **2022**; 18:e1009914.
23. Stone M, Di Germanio C, Wright DJ, et al. Use of US blood donors for national serosurveillance of severe acute respiratory syndrome coronavirus 2 antibodies: basis for an expanded national donor serosurveillance program. *Clin Infect Dis* **2022**; 74:871–81.
24. Ball EE, Weiss CM, Liu H, et al. Severe acute respiratory syndrome coronavirus 2 vasculopathy in a Syrian golden hamster model. *Am J Pathol* **2023**; 193:690–701.
25. Ohsawa K, Imai Y, Sasaki Y, Kohsaka S. Microglia/macrophage-specific protein Iba1 binds to fimbrin and enhances its actin-bundling activity. *J Neurochem* **2004**; 88:844–56.
26. Mantovani A, Sica A, Sozzani S, et al. The chemokine system in diverse forms of macrophage activation and polarization. *Trends Immunol* **2004**; 25:677–86.
27. Waddell A, Ahrens R, Steinbrecher K, et al. Colonic eosinophilic inflammation in experimental colitis is mediated by Ly6C(high) CCR2⁺ inflammatory monocyte/macrophage-derived CCL11. *J Immunol* **2011**; 186:5993–6003.
28. Lawrence T, Natoli G. Transcriptional regulation of macrophage polarization: enabling diversity with identity. *Nat Rev Immunol* **2011**; 11:750–61.
29. Gonzalez-Quintela A, Alende R, Gude F, et al. Serum levels of immunoglobulins (IgG, IgA, IgM) in a general adult population and their relationship with alcohol consumption, smoking and common metabolic abnormalities. *Clin Exp Immunol* **2008**; 151:42–50.
30. Pati S, Fennern E, Holcomb JB, et al. Treating the endotheliopathy of SARS-CoV-2 infection with plasma: lessons learned from optimized trauma resuscitation with blood products. *Transfusion* **2021**; 61(Suppl 1):S336–47.